

Analysis of Macroscopic Cavitation Characteristics of a Self-Excited Oscillating Cavitation Jet Nozzle

Y. Zhao¹, G. Li², F. Zhao³, X. Wang^{3†}, and W. Xu⁴

¹School of the Environment and Safety Engineering, Jiangsu University, Zhenjiang, 212013, China

²Gongqing Institute of Science and Technology, Gongqingcheng Shi, Jiangxi 332020, China

³Research Center of Fluid Machinery Engineering and Technology, Jiangsu University, Zhenjiang 212013, Jiangsu Province, China

⁴School of Energy and Power Engineering, Jiangsu University, Zhenjiang 212013, Jiangsu Province, China

†Corresponding Author Email: 791837776@qq.com

ABSTRACT

The self-excited oscillating cavitation jet nozzle (SEOCJN) serves as a crucial component for converting hydrostatic energy into dynamic pressure energy and ensuring optimal hydraulic and cavitation performance of cavitating jets. Thus, it is of crucial significance to understand the cavitation characteristics and the influence law of SEOCJN for its extensive industrial applications. This paper utilizes numerical simulation methods to analyze the dynamic process of cavitation initiation, development, and outlet cavitation performance of SEOCJN. It explores the effects of inlet pressure and flow rate on the frequency characteristics of SEOCJN, and establishes a mathematical relationship between self-excited oscillation frequency and outlet flow frequency. The results indicate that the self-excited oscillation nozzle has an inlet diameter (D_1) of 4.7 mm, an outlet diameter (D_2) of 12.2 mm, a length (L) of 52 mm, a chamber diameter (D) of 83 mm, an oscillation angle of 120° , and an inlet pressure (P_{in}) of 4.8 MPa. At these parameters, the frequency of the pulse jet reaches 830.01 Hz, with an internal flow period of approximately 0.0024 s. The maximum vapor volume fraction is found to be located 0.28 m from the outlet of the SEOCJN. Furthermore, the frequency of self-excited oscillation pulse increases with an increase in inlet pressure. These findings provide a theoretical basis for the industrial application of self-excited oscillation cavitation jet nozzles.

Article History

Received April 17, 2023

Revised June 18, 2023

Accepted July 3, 2023

Available online September 3, 2023

Keywords:

Self-excited oscillating

Cavitation jet

Inlet pressure

Flow

Self-excitation frequency

1. Introductions

The phenomenon of self-oscillation in fluids is common in nature and engineering. When self-excited oscillation occurs, it often leads to cavitation, sonic boom, coupling, and other related phenomena (Liao et al., 2003; Arthurs & Ziada 2013; Lai & Liao 2013), causing significant damage to mechanical equipment and materials. The most commonly encountered self-excited oscillating nozzles are organ pipe nozzles and Helmholtz nozzles. Due to their simplicity of operation, ease of maintenance, and low investment cost, self-excited oscillation nozzles are widely used in ultra-fast cooling (Thomas 2005; Zhang & Wang 2020), rock breaking in oil drilling (Liu et al., 2014; Lu et al., 2014), organic wastewater treatment (Zhao et al., 2021), and fuel jet

crushing and atomization treatment (Li et al. 2016; Gao et al. 2022). However, the mechanism behind self-excited oscillating pulse jets is still under continuous improvement, and the turbulent flow field inside these nozzles is extremely complex, which significantly restricts their breadth and depth of application.

Currently, significant progress has been made in studying of the performance parameters of self-excited oscillating cavitation jets. Zhang et al. found that the average outlet flow of the self-excited pulse nozzle was lower than that of the cylindrical convergence nozzle, while the instantaneous outlet velocity and dynamic pressure of the self-excited pulse nozzle were higher. They also observed that the self-excited pulse jet increased the turbulent flow intensity and heat flux on the plate surface (Zhang & Wang 2020). Zhao et al. and Li et al. investigated the influence of geometric and external

parameters on the cavitation performance of self-excited oscillation and determined the contribution rate of each parameter to the steam volume fraction (Li et al., 2017; Zhao et al., 2021). Li et al. compared the rock-breaking performance of continuous water jets and self-excited oscillation pulse jets, finding that the latter outperformed the former under the same conditions (Li et al., 2020). Shi et al. studied the cleaning effect of SEOCJN, and found that the cleaning effect was the best when using Helmholtz with organ pipe combination structure (Shi et al., 2022). Wang et al. studied the influence of geometric parameters on the pressure characteristics of self-excited oscillating jets. They observed a sharp decrease in peak pressure with increasing target distance and noted that the peak pressure tended to stabilize beyond a certain range of target distances (Wang et al., 2020). Feng et al. explored the sensitivity of different nozzles to fluids and found that Helmholtz nozzles increased pressure peaks and amplitudes, producing stronger natural vibrations compared to ordinary nozzles (Feng et al., 2022). Li et al. provided a brief introduction to the working principle of self-excited oscillation nozzles, along with experimental results of pressure characteristics and frequency distribution under different environmental pressures. They also studied the transfer law of pressure fluctuations (Li et al., 2003). Zhang et al. analyzed the effects of inlet diameter, chamber diameter, chamber length, reflection angle, and inlet pressure on jet peak velocity, oscillation frequency and cavitation number. They discovered that the oscillation frequency decreased with increasing inlet diameter, chamber diameter, chamber length, and wall reflection angle (Zhang et al., 2021). Li et al. designed and examined the influence of double-chamber nozzle structure on the dynamic characteristics of the jet. They found that the double-chamber nozzle significantly enhanced the cavitation strength, increased the area of the cavitation cloud by 76%, and reduced the shedding time by 90% (Li et al., 2022). Zhang et al. conducted an analysis of the velocity and pressure characteristics of the self-excited oscillating nozzle. They discovered that the periodic expansion and contraction of the low-pressure vortex ring within the nozzle resulted in periodic changes in the pressure at the outlet section of the nozzle (Zhang et al., 2021). Wang et al. investigated the turbulent flow energy, steam volume fraction and vortex growth cycle at the outlet of the new self-excited oscillating jet nozzle. They observed that the peak turbulent flow energy, jet outlet velocity peak, and steam volume fraction peak increased by approximately 10.3%, 14.6%, and 9.1% respectively (Wang et al., 2020). Xiang et al. studied the influence of the outlet protrusion of the upper nozzle on the self-excited oscillation characteristics. They determined that the length of the outlet protrusion of the upper nozzle and the thickness of the nozzle wall needed to be within a specific range to generate the self-oscillating jet (Xiang et al., 2020). Yu et al. designed a new type of reflux self-excited oscillation nozzle, and found that the pulsation frequency was slightly influenced by the confining pressure. Additionally, they found that it decreased with an increase in the length of the oscillation chamber under a certain pressure difference between the inlet and outlet (Yu et al., 2022). Zhang et al. investigated the influence of nozzle length, length-diameter ratio, and

inlet diameter on turbulence effect and atomization efficiency within the nozzle. They determined that turbulent vortices would form in the self-excited oscillation nozzle, thereby enhancing its atomization effect (Zhang et al., 2022). Wu et al. utilized multi-objective particle swarm optimization to optimize the structural parameters of the self-excited oscillation pulse nozzle. They identified a mutually exclusive relationship between the natural frequency and amplitude of the self-excited oscillation pulse nozzle, where an increase in the natural frequency led to a decrease in amplitude (Wu et al., 2022). Bai et al. found the cause of nozzle pressure oscillation and its first location, noting that its oscillation frequency aligned with the self-excited oscillation frequency (Bai et al., 2022). Wang et al. developed a chamber axisymmetric physical model based on the structure of the self-excited oscillation chamber and its geometric parameters. They obtained results concerning cavitation bubble collapse, two-phase distribution in the chamber, turbulent kinetic energy distribution and velocity distribution of the self-excited oscillation pulse jet within 100 ms (Wang et al., 2017).

Based on the aforementioned findings, the current research primarily focuses on the influence of geometric and external parameters on the pressure characteristics, cavitation performance, and jet dynamics characteristics of self-excited oscillating jets. However, there is a lack of research on the self-excited oscillation frequency and its relationship with the outlet flow frequency. This paper centers on the SEOCJN as the research subject, and analyzes the dynamic process of the initial generation, development, and outlet cavitation performance of internal nozzle cavitation. It explores the influence of inlet pressure and flow on the frequency characteristics of SEOCJN, establishes a mathematical relationship between self-excited oscillation frequency and outlet flow frequency, and provides a theoretical foundation for the industrial application of SEOCJN.

2. MODEL CALCULATIONS AND BOUNDARY CONDITIONS

2.1 Computational Model Selection

In this paper, capturing tiny cavitation bubbles is challenging due to the large middle flow velocity and increased internal shear flow within the SEOCJN. The preliminary simulation utilizes the $k-\epsilon$ model, followed by large eddy simulation (LES) to investigate cavitation in the transient process. However, due to the abundance of tiny cavitation bubbles, achieving convergence in the simulation calculations is not straightforward. Hence, the Zwart-Gerber-Belamri model (Zwart et al., 2004; Prabhakar et al., 2022), known for its accuracy in this specific case, is adopted.

2.2 Geometric Model and Grid Information

2.2.1 Geometric model

The overall shape of the numerical simulation of the SEOCJN is shown in Fig. 1. As the fluid enters the nozzle, self-oscillation occurs within the chamber, transitioning

Table 1 Structure parameters of the SEOCJN

Inlet diameter (D ₁ /mm)	Outlet diameter (D ₂ /mm)	Length (L/mm)	Chamber diameter (D/mm)	Oscillation angle (°)
4.7	12.2	52	83	120 (Qu & Chen 2017)

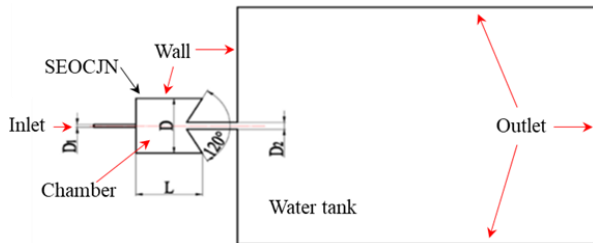


Fig. 1 Structure schematic diagram of the SEOCJN

the flow from continuous to pulsed jet. The velocity of pulsed jet's peak increases in accordance with the self-excitation frequency, thereby intensifying the cavitation effect.

Upon leaving the nozzle, the jet combines with numerous cavitation bubbles, and enters the flooded fluid area. The collapse of these cavitation bubbles generates an extreme environment characterized by high temperature, high pressure and micro-jets (Adhikari et al., 2015; Nan et al., 2018; Xu et al., 2022). The model primarily encompasses five essential parameters, as shown in Table 1.

The high-pressure inlet is positioned at the entrance of the SEOCJN, while the low-pressure inlet corresponds to standard atmospheric pressure. Regarding the outlet boundary conditions, they are applied to the upper, lower, and right sides of the water tank. It is worth noting that the simulation assumes complete submersion of the SEOCJN within the water tank. However, the actual water tank may differ in size from the simulated conditions, and its upper surface should represent a free surface.

2.2.2 Grid Information

In this paper, LES is employed to accurately capture turbulent pulsations at key positions. LES is a simulation method that directly simulates large-scale vortices while modeling the closure of small-scale vortices. It lies between Direct Numerical Simulation (DNS) and Reynolds-Averaged Navier-Stokes (RANS) methods. For turbulence closure in small-scale turbulence the WALE subgrid scale model is utilized. The grid is locally refined, and the refined grid layout is illustrated in Fig. 2.

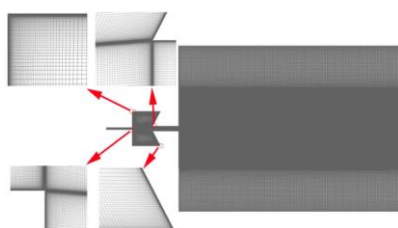


Fig. 2 Grid schematic diagram of the SEOCJN

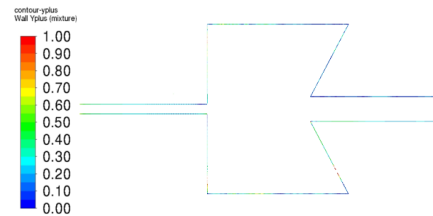


Fig. 3 Cloud diagram of the Y plus of the SEOCJN

The grid is locally refined for both the self-excited cavitation jet nozzle and the water tank. The minimum position value near the wall is set to 0.001 units, and the refinement gradient is applied at the outlet of the SEOCJN to achieve a denser grid in the central area. The grid is slightly less dense on both sides of the tank due to the relatively gentle flow.

2.3 Boundary Conditions

In the numerical simulation process, a pressure-based transient simulation is selected. The time step is set to 1×10^{-6} s, and the total calculation time is set as 1 s. The multiphase flow model utilizes the mixture model. The mixture consists of pure water and water vapor, with the density of pure water defined as 998.2 kg/m^3 , and the viscosity as $1.003 \times 10^{-3} \text{ kg/(m}\cdot\text{s)}$. The density of water vapor is defined as 0.5542 kg/m^3 , and the viscosity as $1.34 \times 10^{-5} \text{ kg/(m}\cdot\text{s)}$. The cavitation model selected is the Zwart-Gerber-Belamri model (Zwart et al., 2004), which considers cavitation as the mass transport mechanism of multiphase flow. The saturated vapor pressure of water is 3540 Pa. The initial inlet pressure is set to 4.8 MPa, and the upper surface of the tank serves as the low-pressure inlet boundary with a set pressure value of 101325 Pa. The outlet boundary is chosen as the outlet of the tank, and the atmospheric pressure value is also set to 101325 Pa.

2.4 Grid independence verification

2.4.1 Y plus

During LES, Y plus is an important parameter for assessing the grid quality and the reasonableness of the boundary layer grid setting. In LES, the boundary layer's Y plus value should be below 1. Figure 3 illustrates the Y plus values in the simulation process. As shown in Fig. 3, the Y plus values are mostly below 1, indicating that the grid meets the requirements for LES calculations (Wang & Chen 2022).

2.4.2 Grid Independence Testing

In LES, it is crucial to consider not only grid refinement but also grid independence to minimize its influence on simulation results, as shown in Fig. 4. From

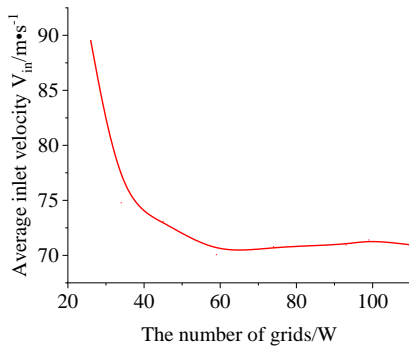


Fig. 4 Relationship between the number of grids and the average inlet velocity

Fig. 4, it is evident that a smaller number of grids leads to a significant error in the simulation results. When the grid count is below 500,000, there is a large deviation in the inlet flow rate. However, when the grid count exceeds 600,000, the number of grids has minimal effect on the flow state. Considering the computational limitations, a grid count of 990,000 is chosen for the simulation.

3. RESULTS AND DISCUSSIONS

3.1 Cavitation Characteristics

3.1.1 Cavitation Initiation

The cavitation number σ is a dimensionless parameter used to describe the cavitation state.

$$\sigma = \frac{P_{\infty} - P_v}{\frac{1}{2} \rho V_{\infty}^2} \quad (1)$$

Where P_{∞} is the pressure of the liquid, P_v is the saturated vapor pressure, ρ is the density of the liquid, V_{∞} is the velocity of the liquid.

Due to the high inlet pressure, a higher flow rate is easily generated, leading to the formation of a velocity shear zone. As a result, the duration of primary cavitation is relatively short, and distinct primary cavitation can be observed at 0.0018 s. Figure 5 (a) and 5(b) demonstrate that primary cavitation predominantly occurs in the middle and front section of the self-oscillating cavitation jet nozzle chamber. This phenomenon arises from the generation of vortex flow due to the shear between the high-speed fluid entering the chamber and the pre-existing low-speed fluid. The lower pressure at the center of the vortex compared to the saturated vapor pressure causes cavitation to form in the vortex core.

From Fig. 5(c), it is evident that the cavitation number significantly decreases by approximately 0.0001 at the location where cavitation occurs. Fig. 5(d) shows the corresponding fluid density, revealing a significant decrease at the cavitation site. Additionally, the primary cavitation assumes an elongated strip shape rather than a circular form. This shape may result from the stretching of cavitation by the high-speed fluid in the middle of the chamber, indicating that cavitation may not appear perfectly round under the influence of the cavitation jet.

3.1.2 Development of Cavitation

Continuous shearing between the incoming high-speed fluid and the fluid in the chamber leads to the ongoing development and aggregation of primary cavitation, gradually forming a sheet-like structure. The cavitation group initially emerges at the edge of the intermediate high-speed fluid and gradually spreads outward, forming the cavitation cloud shown in Fig. 6. Notably, three pairs of symmetrical cavitation clouds appear within the self-excited oscillation chamber. The presence of distinct vortices caused by the shear between high-velocity and low-velocity fluid accounts for this phenomenon, as observed in the velocity and streamline cloud plots in Fig. 6.

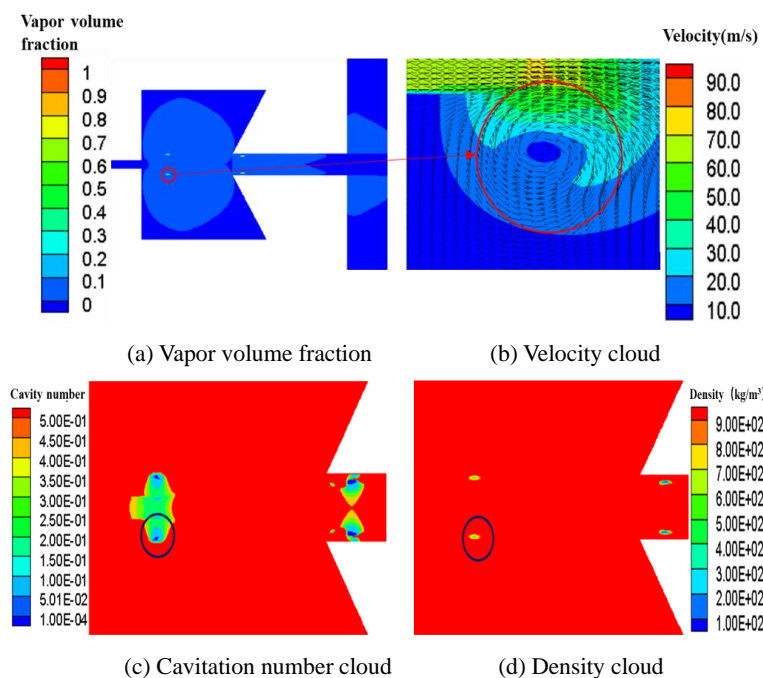


Fig. 5 Primary cavitation cloud diagram of the SEOCJN

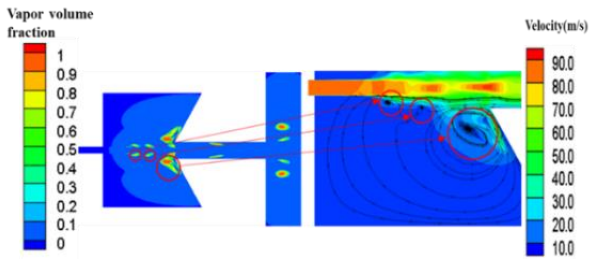


Fig. 6 Vapor volume fraction and velocity cloud diagram of the SEOCJN

Figure 6 clearly illustrates a symmetrical flow field between the upper and lower levels, indicating that the self-oscillation state has not yet transitioned into a self-excited oscillation state within the SEOCJN at this stage. This condition arises from the fact that the fluid has not yet fully engaged in the flow on both sides of the self-oscillating cavitation jet nozzle near the wall, resulting in low velocity in most areas of the chamber on both sides. As the flow further develops, the flow state of the entire field becomes unstable, causing asymmetry in the chamber's flow state and initiating the cavitation development stage.

In order to analyze the cavitation performance during this stage, a monitoring line is positioned in the middle of the outlet section to quantitatively analyze the change in vapor volume fraction, as shown in Fig. 7.

It can be seen from Fig. 7 that at $t = 0.00356$ s, the cavitation bubble reaches the monitoring line for the first time, exhibiting a low average vapor volume fraction of 0.1799% at the interface. This occurrence represents the passage of the primary cavitation bubble. At $t = 0.0058$ s, the average interfacial vapor volume fraction reaches a higher peak of 0.6563%. Notably, a larger cavitation cloud begins to pass through the middle section of the outlet. Finally, at $t = 0.00701$ s, the interface experiences the highest peak of average vapor volume fraction at 0.7375%.

Furthermore, Fig. 7 illustrates the irregular and violent fluctuations in the entire vapor volume fraction as time progresses, ranging from 0 to approximately 0.7%. This behavior indicates the formation of large cavitation bubbles without the establishment of a stable pulse jet within the SEOCJN.

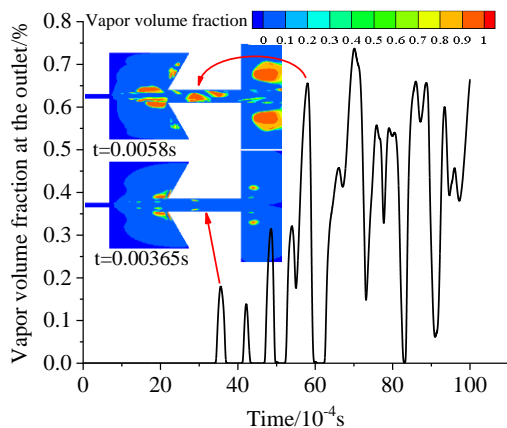


Fig. 7 Variation of vapor volume fraction at the SEOCJN outlet

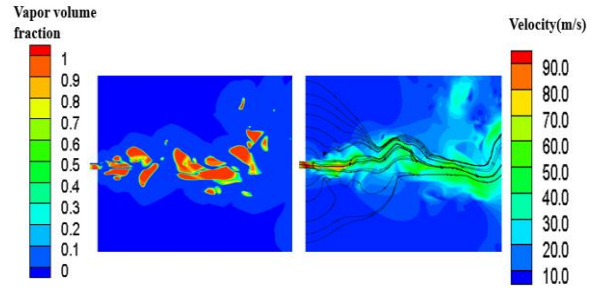


Fig. 8 Vapor volume fraction and velocity cloud diagram in water tank

3.1.3 Analysis of Cavitation Performance at the Outlet of the SEOCJN

The cavitation performance of the flooded self-excited oscillation jet continues to intensify after leaving the nozzle. This is attributed to the high flow rate of the high-speed fluid inside the SEOCJN as it exits the nozzle. Upon entering the tank, the high-speed fluid undergoes shearing with the low-speed fluid present in the stationary tank, further enhancing the cavitation phenomenon. However, as the jet progresses, it gradually encounters hindrance due to the large volume of low-velocity fluid in the tank. As the speed decreases and the pressure rises, a significant number of cavitation bubbles collapse. Fig. 8 illustrates the vapor volume fraction and velocity cloud diagram in the simulated tank at 0.21858 s.

From the vapor volume fraction cloud depicted in Fig. 8, it is evident that as the jet leaves the SEOCJN and enters the water tank, there is a substantial increase in vapor volume fraction. Cavitation bubbles are observed across a considerable area up to a certain distance from the SEOCJN outlet, after which cavitation diminishes.

The velocity cloud plot in Fig. 8 reveals that the majority of the fluid, influenced by the high-speed fluid at the outlet of the self-oscillating cavitation jet nozzle, moves closer to the middle on the low-pressure inlet boundary of the tank. It is attracted and carried forward by the high-speed fluid. Furthermore, the original characteristics of the excitation cavitation jet from the nozzle are nearly indiscernible in the tank. This phenomenon may be attributed to the hindrance caused by the resistance of the low-speed fluid in the tank, leading to the gradual loss of the original oscillation characteristics.

In order to accurately explore the collapse of cavitation-containing fluids after leaving the nozzle as shown in Fig. 9, a monitoring line is established starting 30 mm from the SEOCJN outlet, with a length of 200 mm and increments of 20 mm. Analyzing the change in average vapor volume fraction along the line segment allows for the determination of the collapse pattern of the jet cavitation medium after exiting the nozzle.

Figure 9 illustrates that the average vapor volume fraction gradually increases from the outlet, peaking at a distance of approximately 0.44–0.45 m from the outlet, or roughly 0.28 m from the nozzle exit. This indicates the concentration of a large number of cavitation bubbles at

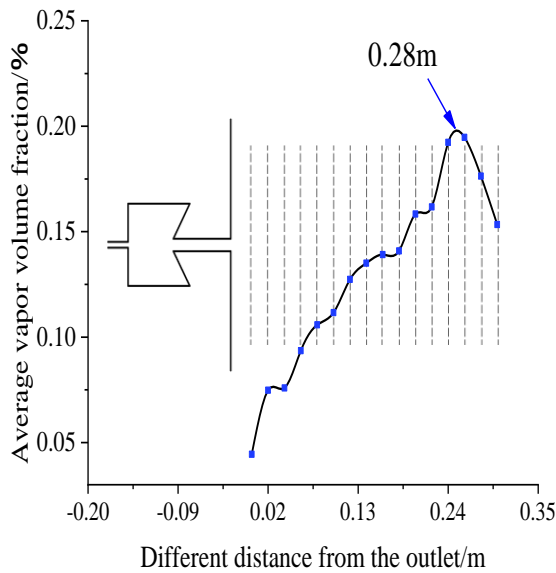


Fig. 9 Average vapor volume fraction at different outlet distances

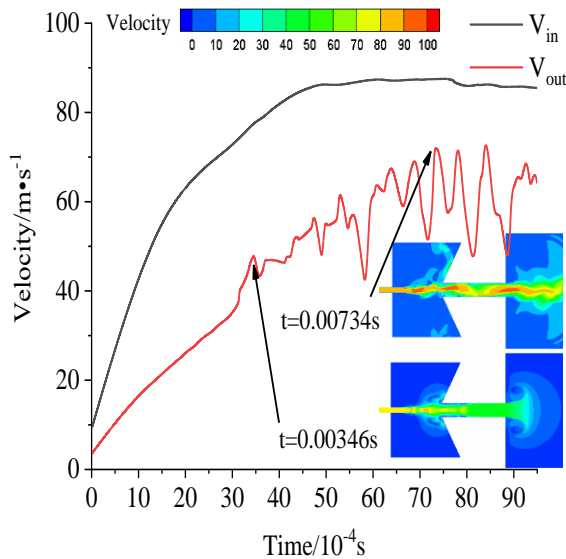


Fig. 10 Variation curve of velocity of the nozzle inlet and outlet with time

this location for collapse. Due to the obstruction of the low-speed fluid in the tank and the influence of complex and variable turbulence, the flow behavior of the mixed fluid becomes less distinguishable, and the cavitation bubbles gradually subside as the flow distance increases. This finding aligns with the conclusions of Li et al. (2003). Additionally, Wang et al. observed that the pressure pulsation amplitude initially increases and then decreases with distance (Wang et al., 2020), indirectly supporting the research findings of this paper.

3.1.4 Changes in Inlet and Outlet Speeds with Time

In order to determine whether the nozzle enters the self-excited oscillation jet state, Fig. 10 shows the average velocity of the nozzle’s inlet and outlet within the first 0.01 s, along with the velocity cloud distribution of key points.

In Fig. 10, it can be observed that the inlet flow rate stabilizes at around 0.005 s, with a consistent speed of approximately 86 m/s. Based on Bernoulli’s equation, neglecting potential energy and converting the inlet’s pressure energy to kinetic energy, the calculated speed is approximately 90 m/s. The outlet velocity fluctuates, with the first fluctuation occurring at 0.00346 s. The velocity cloud reveals that the flow velocity in the middle section experiences short pulses, although the intervals are not uniform. After 0.00246 s, there is another period during which the outlet velocity fluctuates upwards. At around 0.0065 s, the outlet velocity begins to reach its peak and fluctuates in a relatively uniform manner.

The velocity cloud in Fig. 10 at 0.0374 s reveals that the peak average velocity of the outlet is caused by the pulse from the high-speed section leaving the outlet at that moment. The fluid in the middle section also exhibits distinct segments of high-speed and low-speed flow, resulting in an alternating velocity distribution that causes the outlet fluid to be emitted in a pulsed manner.

3.2 Influence of External Factors on the Self-Excited Oscillation Frequency

3.2.1 Inlet Pressure

The inlet pressure plays a crucial role in determining the inlet flow rate, which directly affects the periodicity of the oscillating pulse cavitation jet produced by the nozzle. Thus, the inlet pressure has a significant influence on the frequency of the cavitation jet. To accurately examine the impact of different inlet pressures on the cavitation jet’s frequency during the process of self-excited oscillation, the paper adopts a monitoring line positioned at regular intervals from the nozzle outlet. By analyzing the change in average vapor volume fraction along this monitoring line, the influence of different inlet pressures on the cavitation jet’s frequency can be accurately captured. Furthermore, fast Fourier transform (FFT) transformation of the vapor volume fraction on the monitoring line enables the acquisition of precise frequency information. However, selecting an appropriate monitoring method and location presents a challenge due to the chaotic flow state within the nozzle of the self-excited oscillating cavitation jet, resulting in irregular discrete cavitation flow at the pulsating cavitation jet’s outlet section. If the monitoring method and location are chosen incorrectly, significant errors may arise in the obtained data.

To determine the influence of different inlet pressures on the cavitation jet’s frequency during the self-excited oscillation process, this study investigates the vapor volume fraction at the outlet of the SEOCJN under inlet pressures (P_m) ranging from 1 MPa to 5.5 MPa, as shown in Fig. 11.

Figure 11 demonstrates distinct main frequencies in the frequency domain maps under different inlet pressures. This phenomenon is primarily caused by the periodic changes in vapor volume fraction at the nozzle outlet due to self-excitation. Other frequencies may result from irregular fluctuations caused by the instability of the pulsating cavitation jet flow.

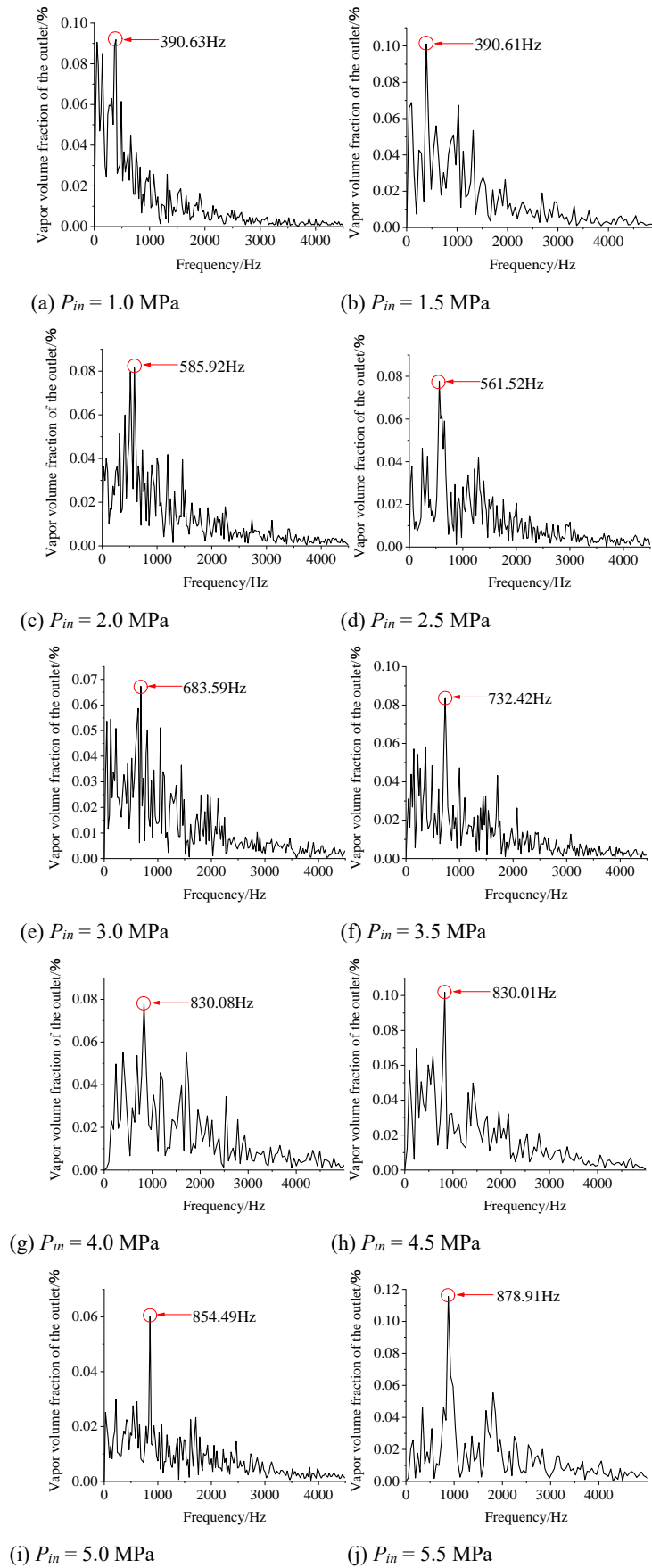


Fig. 11 Frequency-amplitude diagram under different inlet pressure

However, as the peak values of these other frequencies are not significant, they do not impact the main frequency of the jet. Consequently, the main

frequency is plotted as a curve to establish the relationship between the inlet pressure and frequency, as shown in Fig. 12.

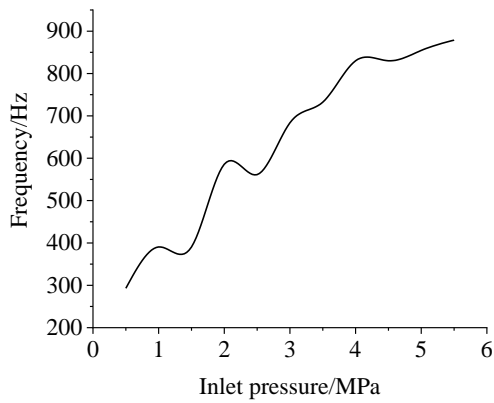


Fig. 12 Influence of different inlet pressures on cavitation frequency

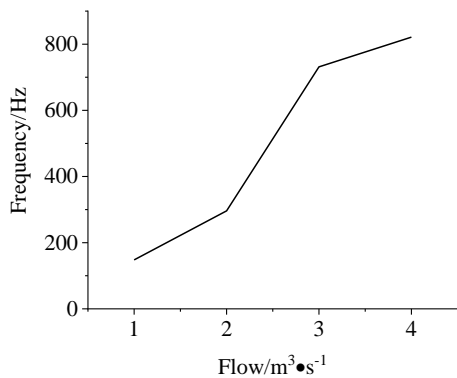


Fig. 13 Diagrams of different flow rates and frequencies

Figure 12 illustrates that the frequency of the self-excited oscillating cavitation jet increases with rising inlet pressure, particularly below 5 MPa. This result aligns with the findings of Lu et al. (2004), with the difference lying in the quantitative analysis presented in this paper. The main reason for this phenomenon is that the inlet pressure directly determines the inlet flow rate, which, in turn, affects the periodicity of the pulse generated by the SEOCJN. Consequently, with a constant chamber size, a higher fluid flow rate leads to a shorter retention time of the fluid within the chamber, resulting in a higher frequency of the corresponding pulse cavitation jet produced by the SEOCJN.

3.2.2 Flow

In order to examine the relationship between flow and the frequency characteristics of the SEOCJN, the model is modified by altering the flow inlet boundary condition while keeping other parameters constant. The simulation calculations are conducted for flow rates ranging from 1 to 4 m³/s, divided into four levels. The results of the simulations are presented in Fig. 13.

Figure 13 illustrates that the inlet flow rate has a clear positive correlation with the frequency of the self-excited oscillating jet. This correlation arises because an increase in flow rate leads to a faster oscillation cycle for the inlet fluid. If the flow rate is too low, the self-oscillation period may not be evident, as most of the environmental noise in the actual process occurs at low frequencies, with weaker intensity compared to high-frequency signals.

3.3 Analysis of the Relationship Between the Self-Excited Oscillation Frequency and the Outlet Flow Frequency

3.3.1 Periodic Analysis of Self-Excited Oscillation Frequency

Due to the high inlet pressure of the nozzle, the large inlet flow rate causes the fluid to enter the self-excited oscillation state rapidly. Figure 14 shows the velocity cloud and streamline diagrams at four key positions. At 0.0076 s in Fig. 14(a), the cloud diagram shows that the flow velocity distribution in the middle part has already started oscillating, followed by the entry of fluid into the lower half of the chamber and the occurrence of a small vortex area at 0.0086 s. Although the oscillation effect is evident at this point, its intensity is not pronounced. In Fig. 14(c), at 0.0098 s, the self-excited oscillating vortex is transferred upward, and a more distinct vortex flow appears in the upper half of the chamber. Notably, high-speed fluid flows directly into the lower half of the chamber upon entering the chamber at 0.011 s, marking the formation of the self-excited oscillation state. For the SEOCJN, when the inlet pressure is 4.8 MPa, the self-excited oscillation effect can be generated relatively quickly, with the distinct self-oscillation phenomenon occurring around 0.011 s.

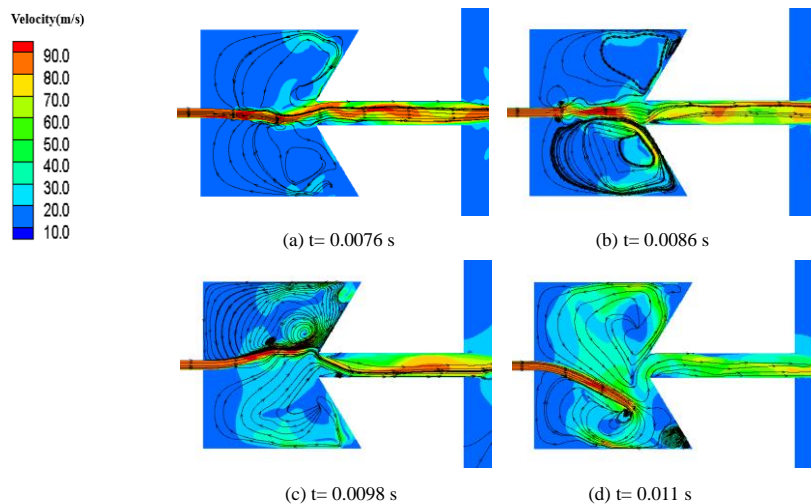


Fig. 14 Velocity cloud diagram in the SEOCJN

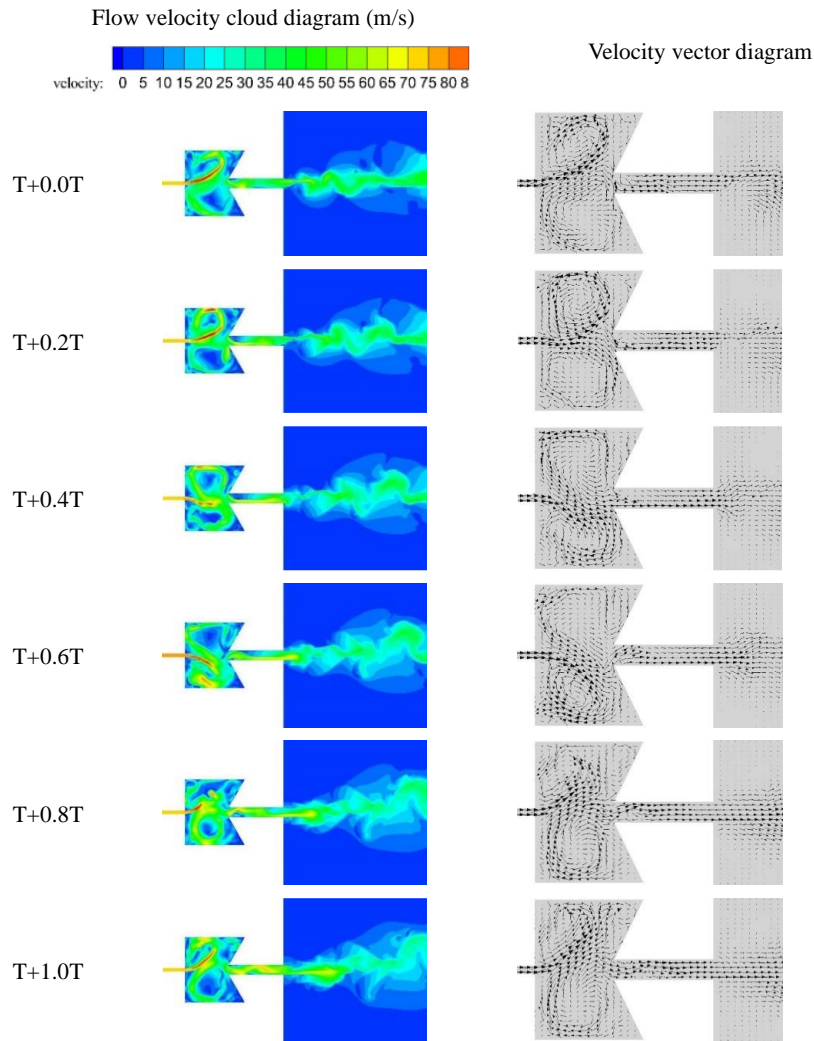


Fig. 15 Velocity cloud diagram and vector diagram of the SEOCJN in a cycle

A more prominent period is selected to analyze the internal flow state of the nozzle during self-excited oscillation. Fig. 15 shows the velocity changes within a cycle from 0.0325 s to 0.0349 s.

From the cloud plot in Fig. 15, it is evident that the fluid flows periodically within the nozzle chamber. Assuming that the high-speed fluid enters the upper half of the chamber as the starting point of the cycle, it fills the upper half of the chamber at 0.2T. At 0.4T, the high-speed fluid exits the upper half and begins to enter the lower half. By 0.6T, the fluid fills the lower half of the chamber, and at 0.8T, it leaves the lower half and starts to enter the upper half again. The fluid completes one cycle by entering the upper half of the cavity at 1T, with a cycle time of approximately 0.0024 s. The vector diagram also indicates fluctuating outlet velocities of the fluid, demonstrating that the fluid is emitted from the self-oscillating cavitation jet nozzle in pulsed form.

To investigate the variation of cavitation groups at the outlet over time, the paper selects a position in the middle of the outlet section, monitors the average vapor volume fraction, and sets the sampling interval to 10^{-5} s. The corresponding results of the monitoring point are shown in Fig. 16 as a cloud map.

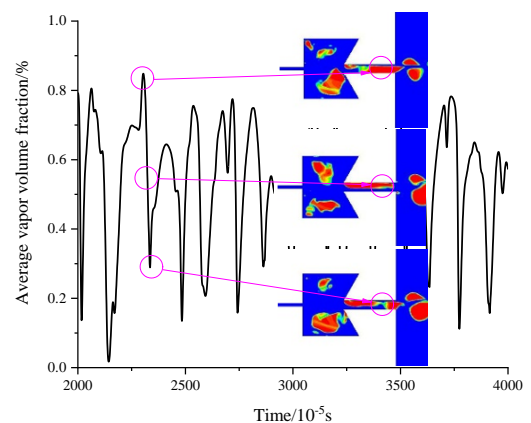


Fig. 16 Vapor volume fraction diagram of the SEOCJN with time

As observed in Fig. 16, the vapor volume fraction at the nozzle outlet exhibits periodic changes over time, which differ from the mentioned cycle. The variation in vapor volume fraction shows a peak at the outlet when the high-speed fluid fills half of the chamber. The pulse period is twice the flow period in the chamber at the jet outlet, indicating that the flow within the chamber contributes to

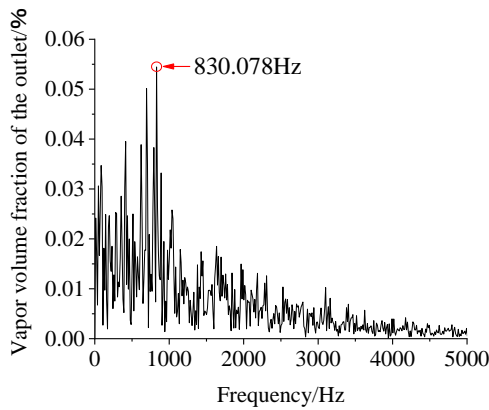


Fig. 17 Cavitation frequency-amplitude diagram of self-excited oscillation jet cavitation nozzle

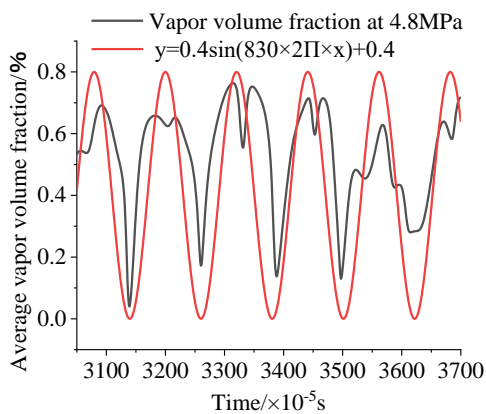


Fig. 18 Comparison of vapor volume fraction of the SEOCJN with standard sinusoidal curve

the generation of a periodic steam-containing fluid jet every half cycle. Consequently, it is apparent that the internal flow characteristics of the nozzle exhibit clear periodicity after the occurrence of self-excited oscillation. As a result of these periodic changes in the internal flow, the fluid velocity at the nozzle outlet also fluctuates periodically.

3.3.2 Analysis of the Outlet Frequency Characteristics of the SEOCJN

Both the velocity of the cavitation jet nozzle and the vapor volume fraction undergo periodic changes. It can be calculated that the flow period within the chamber of the SEOCJN is 0.0024 s. Thus, the analysis focuses on the speed frequency within a single cycle. By computing the flow change frequency in the chamber, based on the flow period in the nozzle chamber, a frequency of 416.67 Hz is obtained. Further analyzing the time variation chart of the vapor volume fraction in Fig. 16 reveals that the change in gas content at the outlet is also periodic.

To extract period and frequency information from the relationship between the vapor volume fraction rate and time, a FFT is employed. This requires subtracting the instantaneous average vapor volume fraction from the overall average and subsequently performing the FFT transformation. Given that the amplitude of the ultra-high-frequency part is nearly zero, it is disregarded during the

analysis. Fig. 17 presents the significant frequency information obtained.

From Fig. 17, the primary frequency of the vapor volume fraction is determined to be 830.078 Hz. Hence, the preliminary explanation is that the pulse frequency of the vapor volume fraction at the nozzle outlet is 830.078 Hz. The average vapor volume fraction at the outlet can be represented by the sinusoidal curve $y = 0.4\sin(830 \times 2\pi x) + 0.4$, constructed with a frequency of 830 Hz. A comparison with the standard sinusoidal curve, as shown in Fig. 18, indicates a near-identical frequency between the two.

The pulse jet frequency of the vapor volume fraction obtained using the fast FFT transformation aligns closely with the simulation results. Converting the frequency of 830.078 Hz to a period of approximately 0.0012 s reveals that the period of the vapor volume fraction at the outlet should be half the flow cycle within the chamber, corresponding to a flow change frequency of 416.67 Hz in the chamber. The pulse jet frequency of 830.078 Hz is almost twice the flow change frequency in the chamber, confirming the consistency with the aforementioned pattern.

4. CONCLUSION

This paper focuses on studying the cavitation effect of the SEOCJN and investigates the influence of inlet pressure and structural parameters on the self-excited oscillating cavitating jet nozzle. The influence of inlet pressure and flow on the frequency characteristics of the SEOCJN is explored, followed by establishing the mathematical relationship between self-excited oscillation frequency and outlet flow frequency. Based on the simulation results, the following conclusions are drawn:

- Inlet pressure enhances the cavitation effect of the model, while the inlet diameter and chamber length of the SEOCJN exert negative influence. Conversely, the outlet diameter of the SEOCJN has a positive influence, and the chamber diameter exhibits no significant effect.
- The internal flow of the SEOCJN demonstrates periodic changes, and the pulse jet frequency at the nozzle outlet correlates with the frequency of internal flow. With an inlet diameter of 4.7 mm, outlet diameter of 12.2 mm, chamber length of 52 mm, chamber diameter of 83 mm, oscillation angle of 120°, and inlet pressure of 4.8 MPa, the SEOCJN achieves a pulse jet frequency of 830.01 Hz, with an internal flow period of approximately 0.0024 s.
- The maximum vapor volume fraction at the outlet of the SEOCJN is 0.28 m. Through numerical simulations employing various inlet pressures, it is observed that the frequency of self-excited oscillation pulses increases with the rise in inlet pressure.

ACKNOWLEDGEMENTS

This work was supported by Key projects of the joint

fund of the National Natural Science Foundation of China (U20A20292); The Fundamental Research Funds for the Central Universities (NO: JZ2021HGB0090); Key R&D Program of Zhenjiang City (GY2020015).

AVAILABILITY OF DATA AND MATERIALS

The datasets used and/or analyzed during the current study are available from the corresponding author upon reasonable request.

CONFLICT OF INTEREST

The authors declare that they have no competing interests.

AUTHORS CONTRIBUTION

Yuanyuan Zhao: Conceptualization; Data collection; Writing the original draft. Guohui Li: data collection; Writing original draft. Fujian Zhao: Writing original draft (Supporting), review and editing. Xiuli Wang: Conceptualization (supporting); writing; review and editing. Wei Xu: Supervision, review and editing.

REFERENCES

- Arthurs, D., & Ziada, S. (2013). Effect of nozzle thickness on the self-excited impinging planar jet. *Journal of Fluids & Structures*, 44(7), 1-16.
- Bai, X., Cao, P. J., Li, Q. L., & Cheng, P. (2022). Generation and transmission mechanisms of disturbance inside injector during self-pulsation. *Acta Aeronautica et Astronautica Sinica*, 43, 126523. <https://doi.org/10.7527/S10006893.2021.26523>.
- Feng, C., Wang, Y., & Kong, L. R. (2022). Effects of pulsating fluid at nozzle inlet on the output characteristics of common and self-excited oscillation nozzle. *Energy Science & Engineering*, 10, 3189-3200. <https://doi.org/10.1002/ese3.1213>
- Li, D., Kong, Y., Ding, X. L., Wang, X. C., & Liu, W. C. (2017). Effects of feeding pipe diameter on the performance of a jet-driven Helmholtz oscillator generating pulsed waterjets. *Journal of Mechanical Science and Technology*, 31(3), 1203-1212. <https://doi.org/10.1007/s12206-017-0219-9>.
- Li, D., Kang, Y., Ding, X. L., Wang, X. H., & Fang, Z. L. (2016). Effects of area discontinuity at nozzle inlet on the characteristics of high speed self-excited oscillation pulsed waterjets. *Experimental Thermal and Fluid Science*, 79, 254-265. <https://doi.org/10.1016/j.exptthermflusci.2016.07.013>
- Li, D. Z., Kang, Y., Shi, H. Q., Hu, Y., Liu, Q., Li, H. C., Hu, J. C., & Li, J. M. (2022). Cavitation cloud dynamic characteristics of dual-chamber self-excited oscillatory waterjet. *Korean Journal of Chemical Engineering*, 39(12), 3214-3226. <https://doi.org/10.1007/s11814-022-1258-1>
- Shi, D. Y., Xing, Y. L., Wang, L. F., & Chen, Z. (2022). Numerical simulation and experimental research of cavitation jets in dual-chamber self-excited oscillating pulsed nozzles. *Shock and Vibration*, <https://doi.org/10.1155/2022/1268288>.
- Zhang, F. B., & Wang, S. (2020). Numerical analysis for jet impingement and heat transfer law of self-excited pulsed nozzle. *ISIJ International*, 60, 2485-2492.
- Zhao, F. J., Wang, X. L., Xu, W., Zhao, Y. Y., Zhao, G. H., & Zhu, H. (2021). Study on different parameters of the self-excited oscillation nozzle for cavitation effect under multiphase mixed transport conditions. *Journal of Marine Science and Engineering*, 9, 1159. <https://doi.org/10.3390/jmse911159>.
- Gao, Y. Q., Zhou, S. Q., Qi, L., & Yin, Q. Q. (2022). Investigation on mechanism breaking fuel jet of self-excited oscillation pulse nozzle. *Journal of Jilin University (Engineering and Technology Edition)*. <https://doi.org/10.13229/j.cnki.jdxbgxb20220960>.
- Li, G. S., Zhang, D. B., Huang, Z. W., Niu, J. L., Zhang, W. W., Gao, G. Q., & An, S. L. (2003). Self-excited oscillating water injection: mechanisms and experiments. *Petroleum Science and Technology*, 21, 145-155. <https://doi.org/10.1081/LFT-120016938>.
- Li, H. S., Liu, S. Y., Jia, J. G., Wang, F. C., & Guo, C. W. (2020). Numerical simulation of rock-breaking under the impact load of self-excited oscillating pulsed waterjet. *Tunnelling and Underground Space Technology*, 96, 103179. <https://doi.org/10.1016/j.tust.2019.103179>.
- Lai, S., & Liao, Z. (2013). The theory and experimental study of the self-excited oscillation pulsed jet nozzle (Pipeline Pulsed Flow Generator). *Natural Resources*, 4(5), 395-403. <https://doi.org/10.4236/nr.2013.45049>.
- Liao, Z., Li, J., Chen, D., Deng, X., Tang, C., & Zhang, F. H. (2003). Theory and experimental study of the self-excited oscillation pulsed jet nozzle. *Chinese Journal of Mechanical Engineering*, 16(4), 379-383. <https://doi.org/10.3901/CJME.2003.04.379>.
- Nan, N., Si, D. Q., & Hu, G. H. (2018). Nanoscale cavitation in perforation of cellular membrane by shock-wave induced nanobubble collapse. *The Journal of Chemical Physics*, 149, 074902. <https://doi.org/10.1063/1.5037643>.
- Prabhakar, K., Srijna, S., & Reddy, S. R. (2022). Assessment of unsteady cavitating flow around modified NACA4412 hydrofoil. *Ocean Engineering*, 266(4), 113039. <https://doi.org/10.1016/j.oceaneng.2022.113039>.
- Liu, S., Liu, Z., Cui, X. X., & Jiang, H. X. (2014). Rock breaking of conical cutter with assistance of front and rear water jet. *Tunnelling and Underground Space Technology*, 42, 78-86. <https://doi.org/10.1016/j.tust.2014.02.002>.
- Zhang, S., Fu, B. W., & Sun, L. (2021). Investigation of the Jet characteristics and pulse mechanism of self-excited oscillating pulsed jet nozzle. *Processes*, 9,

1423. <https://doi.org/10.3390/pr9081423>.
- Thomas, J. K. (2005). *An overview of waterjet fundamentals and applications*. Waterjet Technology Association, St. Louis.
- Adhikari, U., Goliaei, A., & Berkowitz, M. L. (2015). Mechanism of membrane poration by shock wave induced nanobubble collapse: A molecular dynamics study. *Journal of Physical Chemistry B* 119, 6225-6234. <https://doi.org/10.1021/acs.jpcc.5b02218>.
- Wang, X. C., Li, Y. Q., Hu, Y., Ding, X. L., Xiang, M. J., & Li, D. (2020). An experimental study on the jet pressure performance of organ-Helmholtz (o-h), self-excited oscillating nozzles. *Energies*, 13(2), 367. <https://doi.org/10.3390/en13020367>.
- Wang, Z. H., Hu, Y. N., Rao, C. G., & Deng, X. G. (2017). Numerical analysis of cavitation effects of self-excited oscillation pulse nozzles and jet forms. *China Mechanical Engineering*, 28(13), 1535-1541. <https://doi.org/10.3969/j.issn.1004-132X.2017.13.004>.
- Xu, W., Zhu, R. S., Wang, J., Fu, Q., Wang, X. L., Zhao, Y. Y., & Zhao, G. H. (2022). Molecular dynamics simulations of the distance between the cavitation bubble and benzamide wall impacting collapse characteristics. *Journal of Cleaner Production*, 352, 131633. <https://doi.org/10.1016/j.jclepro.2022.131633>.
- Wu, R. Z., Yang, F., Pei, K. C., & Pan, Y. (2022). Structure optimization of self-oscillation pulse nozzle based on multi-objective particle swarm optimization. *Coal Mine Machinery*, 43 (4), 114-116. <https://doi.org/10.13436/j.mkjx.202204036>.
- Xiang, M. J., Wang, X. C., Li, D., Chen, H., & Qian, L. (2020). Effects of Helmholtz upper nozzle outlet structure on jet oscillation characteristics. *Journal of Vibration and Shock*, 39(7), 74-80. <https://doi.org/10.13465/j.cnki.jvs.2020.07.011>.
- Zhang, X. J., Li, X. Q., Nie, S. L., Wang, L. P., & Dong, J. H. (2021). Study on velocity and pressure characteristics of self-excited oscillating nozzle. *Journal of the Brazilian Society of Mechanical Sciences and Engineering*, 5, 43. <https://doi.org/10.1007/s40430-020-02717-4>.
- Lu, Y., Tang, J., Ge, Z., Xia, B., & Liu, Y. (2013). Hard rock drilling technique with abrasive water jet assistance, *International Journal of Rock Mechanics and Mining Sciences* 60, 47-56. <https://doi.org/10.1016/j.ijrmms.2012.12.021>.
- Qu, Y. P., & Chen, S. Y. (2017). Orthogonal experimental research on the structural parameters of a self-excited pulsed cavitation nozzle. *European Journal of Mechanics B/Fluids*. 65, 179-183. <https://doi.org/10.1016/j.euromechflu.2017.03.01>.
- Lu, Y. Y., Li, X. H., & Yang, L. (2004). Effects of gas content in fluid on oscillating frequencies of self-excited oscillation water jets. *Journal of Fluids Engineering*, 126(6), 1058-1061. <https://doi.org/10.1115/1.1839925>.
- Wang, Y., & Chen, X. Z. (2022). Evaluation of wind loads on high-rise buildings at various angles of attack by wall-modeled large-eddy simulation. *Journal of Wind Engineering and Industrial Aerodynamics*, 229, 105160. <https://doi.org/10.1016/j.jweia.2022.105160>.
- Yu, Z. X., Wang, Z. M., Lei, C. B., Zhou, Y. D., & Qiu, X. Q. (2022). Numerical simulation on internal flow field of a self-excited oscillation pulsed jet nozzle with back-flow. *Mechanical Science and Technology for Aerospace Engineering*, 41(7), 998-1002. <https://doi.org/10.13433/j.cnki.1003-8728.20200437>.
- Zhang, Y. Z., Guo, W. Z., Sun, X. H., Shi, J. F., Xue, J. H., & Wang, L. (2022). Structure optimization of mine self-excited oscillation Nozzle based on CFD. *Mining Technology*, 22 (3), 197-200. <https://doi.org/10.13828/j.cnki.ckjs.2022.03.051>.
- Wang, Z. H., Hu, Y. N., Chen, S., Zhou, L., Xu, W. X., & Lien, F. S. (2020). Investigation of self-excited oscillation chamber cavitation effect with special emphasis on wall shape. *Transaction of the Canadian Society for Mechanical Engineering*, 44, 244-255. <https://doi.org/10.1016/j.oceaneng.2022.113039>.
- Zwart, P. J., Gerber, A. G., & Belamri, T. (2004). *A two-phase flow model for predicting cavitation dynamics*. International Conference on Multiphase Flow, Yokohama, Japan.